Pré-Publicações do Departamento de Matemática
Universidade de Coimbra
Preprint Number 14–13

# A COUPLED NON-FICKIAN MODEL OF A CARDIOVASCULAR DRUG DELIVERY SYSTEM

J.A. FERREIRA, J. NAGHIPOOR AND PAULA DE OLIVEIRA

Abstract: A coupled non-Fickian model of a cardiovascular drug delivery system using a biodegradable drug eluting stent is proposed. Energy estimates are used to study the qualitative behaviour of the model. The numerical results are obtained using an IMEX finite element method. The influence of vessel stiffness in the sorption of drug eluted from the stent is analyzed. The results presented in this paper open new perspectives to adapt the drug delivery profile to the needs of the patient.
Keywords: Non-Fickian coupled model, Cardiovascular drug delivery, Drug eluting stent, Numerical simulation.
*Mathematics Subject Classification (2010):* 65M60, 92-08.

## 1. *Introduction*

A stent is a device with the form of a mesh tube which is inserted into a natural body passage to expand its walls and to provide mechanical support for the wounded tissues. Even if stents are widely used in many medical specialities, its most common use is in vascular surgery to reduce stenosis that is the narrowing of the arteries.

A Drug Eluting Stent (DES) is a stent that releases anti-proliferative drug into the arterial wall with a programmed pharmacokinetics. It consists of a metallic stent strut coated with a polymeric layer that encapsulates a therapeutic drug that will act to reduce smooth muscle cell growth and to prevent an inflammatory response which are the predominant causes of neointima proliferation and in-stent restenosis. Biodegradable polymers like polylactic acid (PLA) have become the materials of choice to coat stents while encapsulating the drug ([26]).

The vessel walls of the cardiovascular system are known to display complex mechanical response under physiological conditions. Arterial stiffness is considered as an excellent indicator of cardiovascular morbidity and mortality in a large percentage of the population as referenced in [12]. The coronary artery has different layers. It mainly consist of elastin, which is responsible

Received April 14, 2014.

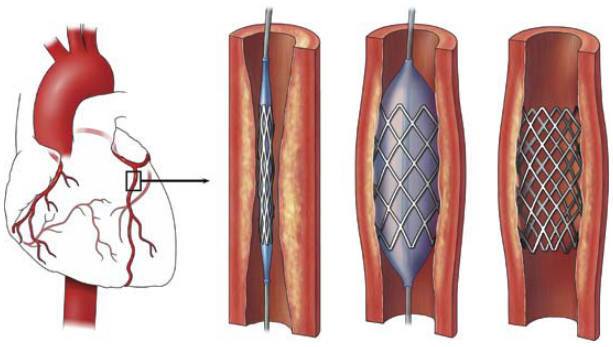

FIGURE 1. Detail of the stented artery, http://www.nucleusmedicalmedia.com.

for the vessel elasticity, combined with collagen. Elastin and collagen are responsible for viscoelastic properties of the vessel. These properties have been clearly demonstrated by laboratorial experiments like creep and relaxation tests [9, 17, 28].

Due to the involvement of so many factors, prediction of drug release appears to be an important issue and mathematical models constitute an important tool to design appropriate drug delivery systems. During the last years, a number of studies have proposed mathematical models for coupled drug delivery in the cardiovascular tissues. We refer without being exhaustive to [3, 5, 10, 14, 15 − 22, 30, 31] and also [23] as a review paper. Most of these studies address the release of drug and its numerical behavior while the viscoelasticity of the vessel wall and the behaviour of the biodegradable materials are disregarded.

In this paper, we propose a non-Fickian coupled model for predicting the biodegradation of PLA as a drug carrier in the coated stent and the simultaneous release of the drug from the coating into the vessel wall. The effect of viscoelasticity of the vessel wall in the drug release is investigated using Maxwell-Wiechert model ([4]).

The geometrical and mechanical effects of the stent strut on degradation and drug release are considered negligible in this paper. As the transport properties through the glycocalyx (the coverage of endothelium) are not well known, we have considered such properties in the endothelium layer.

The paper is organized as follows. Section 2 is devoted to the description of the model and its initial, boundary and interface conditions. In Section 3 we briefly explain the mass behaviour of the materials in a phenomenological approach. In Section 4 we present a variational formulation and prove

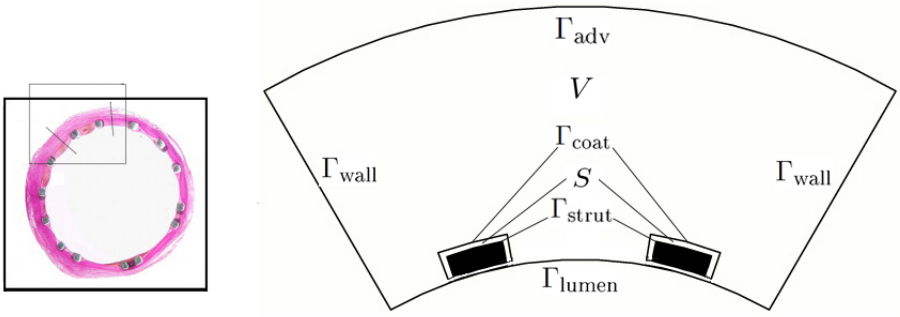


FIGURE 2. Drug eluting stent inside the vessel wall.

a stability result for the continuous model. Using an implicit-explicit finite element method, we establish in Section 5, a discrete form of the stability results. Numerical simulations as well as a sensitivity analysis of the viscoelastic parameters are discussed in section 6. Finally in Section 7, some conclusions are presented.

## 2. *Description of the model*

Three main phenomena explain the kinetics of the drug and the biodegradable polymer: chemical reactions, convection and non-Fickian diffusion.

**2.1.** *Chemical reactions.* When a DES is implanted in a vessel, the coated stent will be gradually covered by neo-intima. For a sake of simplicity, we consider that the drug eluting stent is already inside of the vessel wall (see Figure 2).

Three main reactions are responsible for the degradation of PLA into lactic acid and oligomers, both in the coated stent and in the vessel wall. In the first reaction, the hydrolysis of the PLA occurs resulting in molecules with smaller molecular weights: oligomers (with molecular weight $M_W$ such that $20K \leq M_W \leq 120K$), lactic acid (with molecular weight $M_W \leq 20K$). The second and the third reactions are the hydrolysis of the oligomers resulting in lactic acid occurring in the coating and in the vessel wall respectively. In what follows the subscript $S$ stands for the stent coating while the subscript $V$ stands for the vessel wall (see Table 1).

| Molecule | Stent coating (S) | Vessel wall (V) |
|---|---|---|
| Plasma | $C_{1,S}$ | $C_{1,V}$ |
| PLA | $C_{2,S}$ | - |
| Oligomers | $C_{3,S}$ | $C_{3,V}$ |
| Lactic acid | $C_{4,S}$ | $C_{4,V}$ |
| Drug | $C_{5,S}$ | $C_{5,V}$ |

TABLE 1. Notation for the concentrations.

The previously mentioned reactions are represented schematically by

$$\begin{aligned} &\text{Reaction 1: } C_{1,S} + C_{2,S} \xrightarrow{\kappa_{1,S}} C_{3,S} + C_{4,S}, \\ &\text{Reaction 2: } C_{1,S} + C_{3,S} \xrightarrow{\kappa_{2,S}} C_{4,S}, \\ &\text{Reaction 3: } C_{1,V} + C_{3,V} \xrightarrow{\kappa_{1,V}} C_{4,V}, \end{aligned} \tag{1}$$

where $\kappa_{1,S}$ and $\kappa_{2,S}$ denote the reaction rates of the hydrolysis of PLA and oligomers in the stent and $\kappa_{1,V}$ denotes the reaction rate of the hydrolysis of oligomers in the vessel wall.
The evolution in time and space of each concentration depends on the type of chemical reaction involved: production or consumption reaction. To simplify the presentation of the reaction terms that affect the behaviour of each concentration, we introduce the notations:

$$\mathcal{C}_S = \big(C_{m,S}\big)_{m=1,\dots,5},\ \mathcal{C}_V = \big(C_{m,V}\big)_{\substack{m=1,\dots,5,\\ m\neq 2}} \text{ and } \mathcal{C} = (\mathcal{C}_S, \mathcal{C}_V). \tag{2}$$

where $\mathcal{C}_j,\ j = S, V$ are defined in $(x, y, t) \in \bar{j} \times \mathbb{R}^+$.
Let $F_{m,j}(\mathcal{C}_j),\ m = 1, \dots, 5,\ j = S, V$, be the reaction terms to be considered in the evolution of the concentration. We adopt in what follows the reaction terms introduced in [22] and used in [8] which are defined by

$$F_{m,S}(\mathcal{C}_S) = \begin{cases} -\sum\limits_{i=1,2} \mathcal{F}_{i,S}(\mathcal{C}_S), & \text{m=1,} \\ -\mathcal{F}_{1,S}(\mathcal{C}_S), & \text{m=2,} \\ \sum\limits_{i=1,2} (-1)^{i-1} \mathcal{F}_{i,S}(\mathcal{C}_S), & \text{m=3,} \\ \sum\limits_{i=1,2} \mathcal{F}_{i,S}(\mathcal{C}_S), & \text{m=4,} \\ 0, & \text{m=5,} \end{cases} \tag{3}$$

for the stent and

$$F_{m,V}(\mathcal{C}_V) = \begin{cases} -\mathcal{F}_{1,V}(\mathcal{C}_V), & \text{m=1,} \\ -\mathcal{F}_{1,V}(\mathcal{C}_V), & \text{m=3,} \\ \mathcal{F}_{1,V}(\mathcal{C}_V), & \text{m=4,} \\ 0, & \text{m=5,} \end{cases} \tag{4}$$

for the vessel wall. In (3) and (4) the following definitions are used

$$\begin{array}{l} \mathcal{F}_{1,S}(\mathcal{C}_S) = \kappa_{1,S} C_{1,S} C_{2,S} \big(1 + \alpha C_{4,S}\big), \\ \mathcal{F}_{2,S}(\mathcal{C}_S) = \kappa_{2,S} C_{1,S} C_{3,S} \big(1 + \beta C_{4,S}\big), \\ \mathcal{F}_{1,V}(\mathcal{C}_V) = \kappa_{1,V} C_{1,V} C_{3,V} \big(1 + \gamma C_{4,V}\big), \end{array} \tag{5}$$

where $\alpha$, $\beta$ and $\gamma$ are some positive dimensional constants (see the Annex for more details).

**2.2.** *Convection.* The transport of oligomers, lactic acid and drug in the stent and in the vessel wall occurs by diffusion and convection. The same phenomena occur in the transport of PLA in the stent. The convection is caused by the porous structure of the polymeric matrix and the vessel wall. Let $p_j,\ j = S, V$, represent the pressures in the stent and in the vessel wall respectively and $u_j,\ j = S, V$, be the corresponding velocities. We consider in what follows the geometry described in Figure 2. We also assume that the plasma is incompressible and that its behaviour is described by Darcy's law. The velocities and the pressures then satisfy the following equations

$$\begin{cases} u_V = -\frac{k_V}{\mu_V} \nabla p_V & \text{in } V, \\ \nabla . u_V = 0 & \text{in } V, \\ p_V = p_{lumen} & \text{on } \Gamma_{\text{lumen}}, \\ p_V = p_{adv} & \text{on } \Gamma_{\text{adv}}, \\ u_V . \eta_V = 0 & \text{on } \Gamma_{\text{wall}}, \end{cases} \tag{6}$$

in the vessel wall and

$$\begin{cases} u_S = -\frac{k_S}{\mu_S} \nabla p_S & \text{in } S, \\ \nabla . u_S = 0 & \text{in } S, \\ u_S . \eta_S = 0 & \text{on } \Gamma_{\text{strut}}, \end{cases} \tag{7}$$

in the stent. In (6) and (7), $\eta_j,\ j = S, V$, represents the exterior unit normal. These equations are completed with the matching condition

$$\begin{cases} p_S = p_V & \text{on } \Gamma_{\text{coat}}, \\ u_S . \eta_S = -u_V . \eta_V & \text{on } \Gamma_{\text{coat}}, \end{cases} \tag{8}$$

where the boundaries $\Gamma_{\text{lumen}}$, $\Gamma_{\text{coat}}$, $\Gamma_{\text{strut}}$, $\Gamma_{\text{wall}}$ and $\Gamma_{\text{adv}}$ are defined in Figure 2.
The permeabilities $k_S$ and $k_V$ depend on the properties of the medium and also on the concentrations of PLA, oligomers, lactic acid and drug in the stent and oligomers, lactic acid and drug in the vessel wall. As the functional relations satisfied by $k_j,\ j = S, V$, are not described in the literature, and to simplify the model, we assume that $k_j,\ j = S, V$, are constant. The viscosities $\mu_j, j = S, V$, depend on the chemical compounds present in the stent and in the vessel wall. To simplify, we also assume in what follows that the viscosities are constant.

**2.3.** *Viscoelastic effects.* Viscoelastic models have been widely used to characterize mechanistic properties of the vascular tissues due to its ability to tailor both the viscoelastic relaxation function and the nonlinear elastic stress-strain relation. Numerous viscoelastic models, derived under different experimental conditions, have been proposed in the literature [15 − 17, 26, 27]. In what follows, we present a linear model (*Maxwell-Wiechert* model, [4]). The multiple relaxation times used in this model are well adapted to predict viscoelastic behaviour in living tissues ([17]). We postpone for a later section some considerations on the use of a nonlinear model (*Fung*'s model, [9]).
In the *Maxwell-Wiechert* model, the relation between the stress and the strain is given by the following convolution integral

$$\sigma_V(t) = -\left(k_r\varepsilon_V(t) + \int_0^t K(t-s)\frac{d\varepsilon_V}{ds}(s)ds\right) \text{ in } V, \tag{9}$$

where $\sigma_V$ stands for the stress in the arterial wall, $\varepsilon_V$ is the infinitesimal strain, $\kappa_r$ is the Young modulus of the spring arm and the convolution memory kernel $K$ is defined by $K(t-s) = \sum_{i=1}^{n} \kappa_i e^{-\frac{t-s}{\tau_i}}$, where $\tau_i = \frac{\eta_i}{\kappa_i},\ i = 1, \ldots, n$.
The constants $\kappa_i,\ i = 1, \ldots, n$, represent the Young modulus of the Maxwell arms while $\eta_i,\ i = 1, \ldots, n$, are their viscosities. This means that for $t = 0$ the Young modulus is $\kappa_r + \sum_{i=1}^{n} \kappa_i$ while for $t \to \infty$ its value is $\kappa_r$.
It should be noted that the negative sign in (9) indicates that $\sigma$ and $\varepsilon$ are of opposite sign. This represents the fact that the vessel wall acts like a barrier to the entry of the drug ([7]).
By using integration by parts, $\varepsilon_V(0) = 0$ and assuming a linear relationship

between strain and concentrations in the vessel wall, $\varepsilon_V(t) = \alpha_m C_{m,V}(t),\ m = 1,\dots,5,\ m \neq 2$, we will have

$$\sigma_{m,V}(t) = -\alpha_m\Big((\kappa_r + \sum_{i=1}^{n}\kappa_i)C_{m,V}(t) - \sum_{i=1}^{n}\frac{\kappa_i}{\tau_i}\int_0^t e^{-\frac{t-s}{\tau_i}}C_{m,V}(s)ds\Big) \text{ in } V, \tag{10}$$

for $m = 1,\dots,5,\ m \neq 2$.

Particular attention will be devoted to the case $n = 1$ that is a mechanical analog compound by an elastic arm and a Maxwell arm. If we consider $K(t-s) = \big(\frac{\tau_\sigma}{\tau_1} - 1\big)\kappa_r e^{-\frac{t-s}{\tau_1}}$ for $\tau_1 = \frac{\eta_1}{\kappa_1}$ and $\tau_\sigma = \eta_1\frac{\kappa_1+\kappa_r}{\kappa_1\kappa_r}$, we obtain the so called 3−parameter solid model which can also be deduced from the following differential formulation

$$\sigma_V + \tau_1\frac{\partial\sigma_V}{\partial t} = -\kappa_r\big(\varepsilon_V + \tau_\sigma\frac{\partial\varepsilon_V}{\partial t}\big), \tag{11}$$

where $\sigma_V(0) = \varepsilon_V(0) = 0$. Equation (11) defines one of the simplest linear viscoelastic models that simultaneously captures effects of creep and stress relaxation.

Equation (11) leads to the following formulation

$$\sigma_{m,V}(t) = -\alpha_m\Big(\kappa_r\frac{\tau_\sigma}{\tau_1}C_{m,V}(t) - \frac{\kappa_1}{\tau_1}\int_0^t e^{-\frac{t-s}{\tau_1}}C_{m,V}(s)ds\Big) \text{ in } V,\ m = 1,\dots,5,\ m \neq 2. \tag{12}$$

**2.4.** *The transport of drug: a reaction-diffusion-convection problem.* The reaction-convection-diffusion processes that take place in the stent are then described by the following system of equations

$$\frac{\partial C_{m,S}}{\partial t} = \nabla.\big(D_{m,S}\nabla C_{m,S} - u_S C_{m,S}\big) + F_{m,S}(\mathcal{C}_S) \text{ in } S\times\mathbb{R}^+,\ m = 1,\dots,5, \tag{13}$$

where the meaning of parameters and variables is summarized in Tables 1 and 2 (Annex).

The transport process that occurs in the vessel wall is due to convective transport and non-Fickian diffusion driven by the stress. It is described by the following set of equations

$$\frac{\partial C_{m,V}}{\partial t} = \nabla.\big(\bar{D}_{m,V}\nabla C_{m,V} - u_V C_{m,V}\big) + \nabla.\big(\bar{D}_\sigma\nabla\sigma_{m,V}\big) + F_{m,V}(\mathcal{C}_V) \text{ in } V\times\mathbb{R}^+,\ {}^{m=1,\dots,5,}_{m\neq 2}, \tag{14}$$

where the stress $\sigma_{m,V},\ m = 1,\dots,5,\ m \neq 2$ is given by (10). In (14), $\bar{D}_\sigma$ represents the "weight" of the non-Fickian diffusion and its physical meaning can be found in [7].

In what follows, particular attention will be paid to system (13) and (14) when the viscoelastic behaviour of the vessel wall is described by the 3−parameter

solid model (12). In this case the coupled problem (13) and (14) takes the form

$$\begin{cases} \frac{\partial C_{m,S}}{\partial t} &= \nabla.\big(D_{m,S}\nabla C_{m,S} - u_S C_{m,S}\big) + F_{m,S}(\mathcal{C}_S) \qquad \text{in } S\times\mathbb{R}^+,\ m=1,\dots,5,\\ \frac{\partial C_{m,V}}{\partial t} &= \nabla.\big(D_{m,V}\nabla C_{m,V} - u_V C_{m,V}\big) + F_{m,V}(\mathcal{C}_V)\\ &\quad + \int_0^t e^{-\frac{t-s}{\tau_1}}\nabla.\big(D_{m,\sigma}\nabla C_{m,V}(s)\big)ds \qquad \text{in } V\times\mathbb{R}^+,\ m=1,\dots,5,\ m\neq 2, \end{cases} \tag{15}$$

where $D_{m,V} = \bar{D}_{m,V} - \alpha_m(\kappa_r+\kappa_1)\bar{D}_\sigma$ and $D_{m,\sigma} = \alpha_m\frac{\kappa_1}{\tau_1}\bar{D}_\sigma$ for $m=1,\dots,5,\ m\neq 2$.

To ensure the positivity of the Fickian diffusion coefficient $D_{m,V}$, the diffusion coefficients $\bar{D}_{m,V}$, the Young modulus $\kappa_r$, the parameters $\kappa_1$ and $\alpha_m$ and the viscoelastic diffusion coefficients $\bar{D}_\sigma$ should satisfy the relation $\bar{D}_\sigma < \frac{\bar{D}_{m,V}}{\alpha_m(\kappa_r+\kappa_1)}$. This assumption guarantees that Fickian diffusion dominates the viscoelastic opposition, which is a physical condition for the effective penetration of drug in the vessel wall.

The diffusivities of the oligomers, the lactic acid and the drug will vary during the degradation process [25]. We assume that the diffusion coefficient of each specie in the stent increases exponentially with the degradation of the PLA. In [22, 25] the following expression

$$D_{m,S} = D^0_{m,S}e^{\alpha_{m,S}\frac{C^0_{2,S}-C_{2,S}}{C^0_{2,S}}} \text{ in } S\times\mathbb{R}^+,\ m=1,\dots,5, \tag{16}$$

was proposed where $D^0_{m,S}$ is the diffusion coefficient of the respective species in the unhydrolyzed PLA and $C^0_{2,S}$ is the concentration of the unhydrolyzed polymer at $t=0$. For a sake of simplicity, we assume that the diffusion coefficients in the vessel wall $D_{m,V},\ m=1,\dots,5,\ m\neq 2$, are constant.

To complete the coupled problem, we define in what follows the initial, the boundary and the interface conditions. At the initial time, we assume that the PLA and drug are distributed in the stent uniformly. We also assume that at the initial time no degradation has occurred and consequently neither oligomers nor lactic acid are in the coating. The initial conditions in the coating are then given by

$$\begin{cases} C_{m,S}(0) = 0,\ m=1,3,4,\\ C_{m,S}(0) = 1,\ m=2,5. \end{cases} \tag{17}$$

The initial concentrations in the vessel wall are

$$\begin{cases} C_{1,V}(0) = 1,\\ C_{m,V}(0) = 0,\ m=3,4,5. \end{cases} \tag{18}$$

We represent by $J_{m,S}$ and $J_{m,V}$ the mass fluxes in the stent and in the vessel wall defined respectively by

$$\begin{aligned} J_{m,S} &= -D_{m,S}\nabla C_{m,S} + u_S C_{m,S} && \text{in } S\times\mathbb{R}^+,\ m=1,\dots,5,\\ J_{m,V} &= -D_{m,V}\nabla C_{m,V} + u_V C_{m,V} - D_{m,\sigma}\int_0^t e^{-\frac{t-s}{\tau_1}}\nabla C_{m,V}(s)ds && \text{in } V\times\mathbb{R}^+,\ {}^{m=1,\dots,5,}_{m\neq 2}. \end{aligned} \tag{19}$$

As the metallic stent strut is impermeable to the drug and PLA degradation products that diffuse in coating stent, no mass flux passes through the boundary surface $\Gamma_{\text{strut}}$. So

$$J_{m,S}.\eta_S = 0 \text{ on } \Gamma_{\text{strut}}\times\mathbb{R}^+,\ m=1,\dots,5. \tag{20}$$

The interface conditions on the interface boundary $\Gamma_{\text{coat}}$ are described by

$$\begin{cases} C_{m,S} = C_{m,V} & \text{on } \Gamma_{\text{coat}}\times\mathbb{R}^+,\\ J_{m,S}.\eta_S = -J_{m,V}.\eta_V & \text{on } \Gamma_{\text{coat}}\times\mathbb{R}^+ \end{cases} \tag{21}$$

for $m=1,\dots,5,\ m\neq 2$. The first condition in (21) represents the continuity of the concentration while the second condition is the continuity of local fluxes.
We recall that the subscript $m=2$ refers to PLA. In equation (21), the interface conditions do not apply to PLA. In fact PLA has a large molecular weight ($M_W \geq 120K$) compared to the other molecules present in the process and consequently it will not cross $\Gamma_{\text{coat}}$. As a result, $\Gamma_{\text{coat}}$ is impermeable to PLA and we assume that $J_{2,S}.\eta_S = 0$. The symmetric boundaries of the vessel wall, $\Gamma_{\text{wall}}$ are sufficiently far away from the domain of interest and a symmetry condition implies no-flux, $J_{m,V}.\eta_V = 0$ for $m=1,\dots,5,\ m\neq 2$. We also assume that $\Gamma_{\text{adv}}$ is impermeable to all molecules.
Since the drug, the oligomers and the lactic acid go directly from the arterial wall to the blood and are transported very fast away from the region of interest, we consider $J_{m,V}.\eta_V = -\gamma_{m,V}C_{m,V},\ m=3,4,5$, for the lumen boundary $\Gamma_{\text{lumen}}$, with an high transference rate $\gamma_{m,V}$. As the plasma penetrates from the blood artery into the arterial wall, we may consider a natural boundary condition $J_{1,V}.\eta_V = \gamma_{1,V}(1-C_{1,V})$ for the plasma.
Summarizing boundary and interface conditions, we have:

$$\begin{cases} J_{m,S}.\eta_S = 0 & \text{on } \Gamma_{\text{strut}}\times\mathbb{R}^+,\ m=1,\dots,5,\\ J_{2,S}.\eta_S = 0 & \text{on } \Gamma_{\text{coat}}\times\mathbb{R}^+,\\ C_{m,S} = C_{m,V} & \text{on } \Gamma_{\text{coat}}\times\mathbb{R}^+,\ m=1,\dots,5,\ m\neq 2,\\ J_{m,S}.\eta_S = -J_{m,V}.\eta_V & \text{on } \Gamma_{\text{coat}}\times\mathbb{R}^+,\ m=1,\dots,5,\ m\neq 2,\\ J_{1,V}.\eta_V = \gamma_{1,V}(1-C_{1,V}) & \text{on } \Gamma_{\text{lumen}}\times\mathbb{R}^+,\\ J_{m,V}.\eta_V = -\gamma_{m,V}C_{m,V} & \text{on } \Gamma_{\text{lumen}}\times\mathbb{R}^+,\ m=3,4,5,\\ J_{m,V}.\eta_V = 0 & \text{on } (\Gamma_{\text{wall}}\cup\Gamma_{\text{adv}})\times\mathbb{R}^+, m=1,\dots,5,\ m\neq 2. \end{cases} \tag{22}$$

## 3. *Qualitative behaviour of the total mass of the system*

In what follows we analyse the behaviour of the total mass of species in the model. We consider

$$\mathcal{M}(t) = \int_S \mathcal{C}_S dS + \int_V \mathcal{C}_V dV, \tag{23}$$

where $\displaystyle\int_S \mathcal{C}_S dS = \sum_{m=1}^{5} \int_S C_{m,S} dS$ and $\displaystyle\int_V \mathcal{C}_V dV = \sum_{\substack{m=1 \\ m\neq 2}}^{5} \int_V C_{m,V} dV$.

Using (15), we obtain

$$\begin{aligned}
\mathcal{M}'(t) \; &= \sum_{m=1}^{5} \int_S \nabla.\big(D_{m,S}\nabla C_{m,S} - u_S C_{m,S}\big) dS + \sum_{m=1}^{5} \int_S F_{m,S}(\mathcal{C}_S) dS \\
&+ \sum_{\substack{m=1 \\ m\neq 2}}^{5} \int_V \nabla.\big(D_{m,V}\nabla C_{m,V} - u_V C_{m,V}\big) dV + \sum_{\substack{m=1 \\ m\neq 2}}^{5} \int_V F_{m,V}(\mathcal{C}_V) dV \\
&+ \sum_{\substack{m=1 \\ m\neq 2}}^{5} \int_V \int_0^t e^{-\frac{t-s}{\tau_1}} \nabla.\big(D_{m,\sigma}\nabla C_{m,V}(s)\big) ds dV.
\end{aligned}$$

Integrating over space and applying external boundary conditions, we have

$$\begin{aligned}
\mathcal{M}'(t) \; &= \sum_{\substack{m=1 \\ m\neq 2}}^{5} \int_{\Gamma_{\text{coat}}} J_{m,S}.\eta_S ds + \sum_{\substack{m=1 \\ m\neq 2}}^{5} \int_{\Gamma_{\text{coat}}} J_{m,V}.\eta_V ds + \int_S \sum_{m=1}^{5} F_{m,S}(\mathcal{C}_S) dS \\
&+ \int_V \sum_{\substack{m=1 \\ m\neq 2}}^{5} F_{m,V}(\mathcal{C}_V) dV + \gamma_{1,V} \int_{\Gamma_{\text{lumen}}} (1 - C_{1,V}) ds - \sum_{m=3}^{5} \gamma_{m,V} \int_{\Gamma_{\text{lumen}}} C_{m,V} ds.
\end{aligned}$$

Let

$$\begin{aligned}
\Delta M_{\Gamma_{\text{lumen}}}(t) &= \sum_{\substack{m=1 \\ m\neq 2}}^{5} \gamma_{m,V} \int_{\Gamma_{\text{lumen}}} C_{m,V}(t) ds, \\
\Delta M_H(t) &= \int_S \kappa_{2,S} C_{1,S}(t) C_{3,S}(t)(1 + \beta C_{4,S}(t)) dS + \int_V \kappa_{1,V} C_{1,V}(t) C_{3,V}(t)\big(1 + \gamma C_{4,V}(t)\big) dV.
\end{aligned} \tag{24}$$

We note that $\Delta M_{\Gamma_{\text{lumen}}}(t)$ represents the mass per unit time of molecules (except PLA) that enters in $\Gamma_{\text{lumen}}$ at the instant $t$ while $\Delta M_H(t)$ stands for the total mass of hydrolyzed oligomers that enter per unit time in the stent

and the vessel wall at the same instant.
Using interface condition on $\Gamma_{\text{coat}}$ we easily establish

$$\mathcal{M}(t) \ = \mathcal{M}(0) + \gamma_{1,V}\left|\Gamma_{\text{lumen}}\right| t - \int_0^t \Delta M_H(\mu) d\mu - \int_0^t \Delta M_{\Gamma_{\text{lumen}}}(\mu)\, d\mu.$$

This last equation means that the total mass in the system at a certain time $t$, $t \in [0, T]$, is given by the difference between the initial mass added with the mass of plasma that enters in the system until time $t$ and the cumulative masses of molecules in $\Gamma_{\text{lumen}}$, the stent and the vessel wall.

## 4. *Weak formulation*

In this section, we introduce a variational form of the initial boundary value problem (15) − (18) and (22).
Let $\Omega$ be a bounded domain in $\mathbb{R}^2$ with boundary $\partial\Omega$. We denote by $L^2(\Omega)$ and $H^1(\Omega)$ the usual Sobolev spaces endowed with the usual inner products $(.,.)$ and $(.,.)_1$ and norms $\|.\|_{L^2(\Omega)}$ and $\|.\|_{H^1(\Omega)}$ respectively. We represent by $L^\infty(\Omega)$ the space of functions $v : \Omega \longrightarrow \mathbb{R}$ such that $\left\|v\right\|_{L^\infty(\Omega)} = \text{ess sup}_\Omega\, |v| < \infty$. The space of functions $v : (0, T) \longrightarrow H^1(\Omega)$ such that $\int_0^T \left\|v(t)\right\|^2_{H^1(\Omega)} dt < \infty$ will be denoted by $L^2(0, T; H^1(\Omega))$ while $L^\infty(0, T; L^\infty(\Omega))$ represents the space of functions $v : (0, T) \longrightarrow L^\infty(\Omega)$ such that $\text{ess}\sup_{(0,T)} \left\|v(t)\right\|_{L^\infty(\Omega)} < \infty$.

**4.1.** *Porous media problem.* In order to find the pressure drop in the stented vessel wall, as $k_j$ and $\mu_j$, $j = S, V$, are constants, it is convenient to rewrite the equations (6) − (8) in terms of pressure drop in the following coupled form

$$\begin{cases} -\nabla.(\frac{k_V}{\mu_V}\nabla p_V) = 0 & \text{in } V, \\ -\nabla.(\frac{k_S}{\mu_S}\nabla p_S) = 0 & \text{in } S, \\ p_V = p_{\text{lumen}} & \text{on } \Gamma_{\text{lumen}}, \\ p_V = p_{\text{adv}} & \text{on } \Gamma_{\text{adv}}, \\ \frac{k_V}{\mu_V}\nabla p_V.\eta_V = 0 & \text{on } \Gamma_{\text{wall}}, \\ p_V = p_S & \text{on } \Gamma_{\text{coat}}, \\ \frac{k_V}{\mu_V}\nabla p_V.\eta_V = -\frac{k_S}{\mu_S}\nabla p_S.\eta_S & \text{on } \Gamma_{\text{coat}}, \\ \frac{k_S}{\mu_S}\nabla p_S.\eta_S = 0 & \text{on } \Gamma_{\text{strut}}. \end{cases} \tag{25}$$

For a sake of simplicity, we assume $p_{\text{adv}} = 0$ and a nonzero pressure $p_{\text{lumen}} = p_0$.
In what follows we use the notations

$$\mathcal{A}_j(p_j, q_j) = \left(\frac{\kappa_j}{\mu_j}\nabla p_j, \nabla q_j\right)_j,\ j = S, V, \tag{26}$$

and we use the following spaces

$$H^1_{\text{lumen}}(V) = \left\{\vartheta \in H^1(V) \text{ such that } \vartheta = 0 \text{ on } \Gamma_{\text{lumen}}\right\} \tag{27}$$

and

$$\mathcal{V} = \left\{(p_S, p_V) \in H^1(S) \times H^1_{\text{lumen}}(V) \text{ such that } p_S = p_V \text{ on } \Gamma_{\text{coat}}\right\}. \tag{28}$$

Let $w \in H^1(V)$ be such that $w = p_{\text{lumen}}$ on $\Gamma_{\text{lumen}}$ and $p_V^* = p_V - w \in H^1_{\text{lumen}}(V)$.
With the previous notations, we consider the weak formulation of problem (25):
Find $(p_S, p_V^*) \in \mathcal{V}$ such that

$$\mathcal{A}_S(p_S, q_S) + \mathcal{A}_V(p_V^*, q_V) = -\mathcal{A}_V(w, q_V),\ \ \forall\ (q_S, q_V) \in \mathcal{V}. \tag{29}$$

It is obvious that $p_V$ can be recovered by $p_V = p_V^* + w$.

**4.2.** *Convection-diffusion-reaction problem.* We adopt in what follows the following notations:

$$\begin{aligned}
&a_S\big(v_S(t), w_S\big) = \Big(D_{m,S}\nabla v_{m,S}(t) - u_S v_{m,S}(t), \nabla w_{m,S}\Big)_S,\\
&a_V\big(v_V(t), w_V\big) = \Big(D_{m,V}\nabla v_{m,V}(t) - u_V v_{m,V}(t), \nabla w_{m,V}\Big)_V + \int_0^t e^{-\frac{t-s}{\tau_1}}\Big(D_{m,\sigma}\nabla v_{m,V}(s), \nabla w_{m,V}\Big)_V ds,\\
&a_{\text{lumen}}(v_V(t), w_V) = \gamma_{1,V}\Big(1 - v_{1,V}(t), w_{1,V}\Big)_{\Gamma_{\text{lumen}}} - \sum_{m=3}^{5}\gamma_{m,V}\Big(v_{m,V}(t), w_{m,V}\Big)_{\Gamma_{\text{lumen}}}.
\end{aligned} \tag{30}$$

These bilinear forms are defined in the Sobolev space

$$\mathcal{W} = \left\{(v_S, v_V) \in \Big(H^1(S)\Big)^5 \times \Big(H^1(V)\Big)^4 \text{ such that } v_{m,S} = v_{m,V} \text{ on } \Gamma_{\text{coat}},\ m = 1, 3, 4, 5\right\}, \tag{31}$$

where $\big(v_S, v_V\big) = \left(\big(v_{m,S}\big)_{m=1,\dots,5}, \big(v_{m,V}\big)_{\substack{m=1,\dots,5\\ m\neq 2}}\right)$ and

$$L^2(0,T,\mathcal{W}) = \left\{\big(w_S, w_V\big) \text{ such that } w_j : (0,T) \longrightarrow \mathcal{W} \text{ and } \int_0^T \big\|w_j(t)\big\|^2_{H^1(j)} dt < \infty,\ j = S, V\right\}. \tag{32}$$

The weak solution of the problem $(15) - (18)$ and (22) is the solution of the following variational problem:

Find $\big(\mathcal{C}_S, \mathcal{C}_V\big) \in L^2(0,T,\mathcal{W})$ such that $\big(\frac{\partial \mathcal{C}_S}{\partial t}, \frac{\partial \mathcal{C}_V}{\partial t}\big) \in \Big(L^2(0,T,L^2(S))\Big)^5 \times \Big(L^2(0,T,L^2(V))\Big)^4$ and

$$\begin{cases} \sum\limits_{j=S,V} \Big( \big(\frac{\partial \mathcal{C}_j}{\partial t}(t), v_j\big)_j + a_j\big(\mathcal{C}_j(t), v_j\big) \Big) = \sum\limits_{j=S,V} \big(\mathcal{F}_j(\mathcal{C}_j(t)), v_j\big)_j + a_{\text{lumen}}(\mathcal{C}_V(t), v_V), \\ \text{a.e in } (0,T), \text{ for all } (v_S, v_V) \in \mathcal{W}, \\ \mathcal{C}_S(0) = (0,1,0,0,1),\ \mathcal{C}_V(0) = (1,0,0,0), \end{cases} \tag{33}$$

where $\mathcal{C}_S$ and $\mathcal{C}_V$ are defined in (2) and

$$\big(\mathcal{F}_S(\mathcal{C}_S), \mathcal{F}_V(\mathcal{C}_V)\big) = \Big( \big(F_{m,S}(\mathcal{C}_S)\big)_{m=1,\dots,5}, \big(F_{m,V}(\mathcal{C}_V)\big)_{\substack{m=1,\dots,5 \\ m\neq 2}} \Big) \tag{34}$$

is defined by (3)-(5).
We define the energy functional

$$\mathcal{E}(t) = \sum_{j=S,V} \Big( \Big\| \mathcal{C}_j(t) \Big\|^2_{L^2(j)} + \int_0^t \Big\| \nabla \mathcal{C}_j(s) \Big\|^2_{L^2(j)} ds \Big) + \Big\| \int_0^t e^{-\frac{t-s}{\tau_1}} \nabla \mathcal{C}_V(s) ds \Big\|^2_{L^2(V)}, \ t \in [0,T], \tag{35}$$

where

$$\Big\| \mathcal{C}_S(t) \Big\|_{L^2(S)} = \sum_{m=1}^{5} \Big\| C_{m,S}(t) \Big\|_{L^2(S)} \text{ and } \Big\| \mathcal{C}_V(t) \Big\|_{L^2(V)} = \sum_{\substack{m=1 \\ m\neq 2}}^{5} \Big\| C_{m,V}(t) \Big\|_{L^2(V)} \cdot \tag{36}$$

An upper bound for the energy functional (35) is established in the following theorem. n the following, the space $L^\infty(0,T,L^\infty(\Omega))$ will be represented by $L^\infty(L^\infty)$.

**Theorem 4.1.** *If* $(\mathcal{C}_S, \mathcal{C}_V) \in L^2(0,T,\mathcal{W})$ *and* $(\frac{\partial \mathcal{C}_S}{\partial t}, \frac{\partial \mathcal{C}_V}{\partial t}) \in \Big(L^2(0,T;L^2(S))\Big)^5 \times \Big(L^2(0,T;L^2(V))\Big)^4$ *is a solution of the variational problem* (33)*, then assuming* $\big(\mathcal{C}_S(t), \mathcal{C}_V(t)\big) \in \big(H^2(S)\big)^5 \times \big(H^2(V)\big)^4$ *we have*

$$\mathcal{E}(t) \ \leq \frac{1}{\min\big\{1, \phi, D_\sigma\big\}} e^{2(\mathcal{K}+\varphi)t} \mathcal{E}(0) + \frac{\gamma_{1,V}}{2} \big|\Gamma_{lumen}\big|^2 \Big( e^{2(\mathcal{K}+\varphi)t} - 1 \Big), \tag{37}$$

*where* $\mathcal{K}, \phi, \varphi$ *and* $D_\sigma$ *are concentration-independent constants while* $|\Gamma_{lumen}|$ *is the length of the transition layer* $\Gamma_{lumen}$*.*

*Proof*: Taking in (33), $v_j = \mathcal{C}_j(t),\ j = S, V$, using (30), (34) and (36), the equality

$$\begin{aligned}\frac{d}{dt}\left\|\int_0^t e^{-\frac{t-s}{\tau_1}}\nabla\mathcal{C}_V(s)ds\right\|^2_{L^2(V)} &= 2\int_0^t e^{-\frac{t-s}{\tau_1}}\Big(\nabla\mathcal{C}_V(s),\nabla\mathcal{C}_V(t)\Big)_V ds\\ &\quad -\frac{2}{\tau_1}\left\|\int_0^t e^{-\frac{t-s}{\tau_1}}\nabla\mathcal{C}_V(s)ds\right\|^2_{L^2(V)},\end{aligned} \tag{38}$$

and the inequalities

$$\Big(u_j\mathcal{C}_j(t),\nabla\mathcal{C}_j(t)\Big)_j \le \big\|u_j\big\|_\infty\left(\varepsilon_j^2\left\|\mathcal{C}_j(t)\right\|^2_{L^2(j)} + \tfrac{1}{4\varepsilon_j^2}\left\|\nabla\mathcal{C}_j(t)\right\|^2_{L^2(j)}\right), \tag{39}$$

for $j = S, V$ that hold for arbitrary positive $\varepsilon_j$, we can establish the following differential inequality

$$\begin{aligned}&\tfrac{1}{2}\tfrac{d}{dt}\sum_{j=S,V}\left(\left\|\mathcal{C}_j(t)\right\|^2_{L^2(j)} + \phi\int_0^t\left\|\nabla\mathcal{C}_j(s)\right\|^2_{L^2(j)}ds + D_\sigma\left\|\int_0^t e^{-\frac{t-s}{\tau_1}}\nabla\mathcal{C}_V(s)ds\right\|^2_{L^2(V)}\right)\\ &\le \sum_{j=S,V}\big\|u_j\big\|_\infty\varepsilon_j^2\left\|\mathcal{C}_j(t)\right\|^2_{L^2(j)} - \tfrac{D_\sigma}{\tau_1}\left\|\int_0^t e^{-\frac{t-s}{\tau_1}}\nabla\mathcal{C}_V(s)ds\right\|^2_{L^2(V)} + \sum_{j=S,V}\big(\mathcal{F}_j(\mathcal{C}_j(t),\mathcal{C}_j(t)\big)_j + \lambda_{\text{lumen}}.\end{aligned} \tag{40}$$

In (40), $\lambda_{\text{lumen}} = \frac{\gamma_{1,V}}{4}\big|\Gamma_{\text{lumen}}\big|^2 - \frac{3\gamma_{1,V}}{4}\left\|C_{1,V}(t)\right\|^2_{\Gamma_{\text{lumen}}} - \sum_{m=3}^{5}\gamma_{m,V}\left\|C_{m,V}(t)\right\|^2_{\Gamma_{\text{lumen}}}$ and

$$\begin{cases}\phi = \min\limits_{j=S,V}\big\{2D_j - \frac{\left\|u_j\right\|_\infty}{2\varepsilon_j^2}\big\},\\ D_S = \min\limits_{m=1,\dots,5}\big\{D_{m,S}\big\},\\ D_V = \min\limits_{\substack{m=1,\dots,5\\ m\neq 2}}\big\{D_{m,V}\big\},\\ D_\sigma = \min\limits_{\substack{m=1,\dots,5\\ m\neq 2}}\big\{D_{m,\sigma}\big\}.\end{cases} \tag{41}$$

It should be noted that $\varepsilon_j$ in (40) should be such that $\varepsilon_j \ge \sqrt{\frac{\left\|u_j\right\|_\infty}{4D_j}},\ j = S, V$. As $H^2(j),\ j = S, V$ are embedded in the space of continuous bounded functions, (see [2]), it can be shown that there exist positive constants $\mathcal{K}_j,\ j = S, V$, depending on $\|\mathcal{C}_j\|_{L^\infty(L^\infty)}$ such that

$$\big(\mathcal{F}_j(\mathcal{C}_j(t),\mathcal{C}_j(t)\big)_j \le \mathcal{K}_j\left\|\mathcal{C}_j(t)\right\|^2_{L^2(j)} \le \mathcal{K}\left\|\mathcal{C}_j(t)\right\|^2_{L^2(j)}. \tag{42}$$

where $\mathcal{K} = \max_{j=S,V} \{\mathcal{K}_j\}$.
By replacing (42) in (40) and taking

$$\varphi = \max_{j=S,V} \{\varepsilon_j^2 \|u_j\|_\infty\}, \tag{43}$$

in differential inequality (40), we consequently deduce

$$\mathcal{E}(t) \leq \frac{1}{\min\{1,\phi,D_\sigma\}} e^{2(\mathcal{K}+\varphi)t}\mathcal{E}(0) + \frac{\gamma_{1,V}}{2}\left|\Gamma_{\text{lumen}}\right|^2\left(e^{2(\mathcal{K}+\varphi)t} - 1\right). \tag{44}$$

■

Estimate (44) proves the stability of the model for finite intervals of time.

## 5. *Finite dimensional approximation*

To define a finite dimensional approximation for the solution of (15) – (18) and (22), we fix $h > 0$ and we define in $\Omega = S \cup V$ (Figure 2) an admissible triangulation $\mathcal{T}_h$, depending on $h > 0$, such that the corresponding admissible triangulations in $S$ and $V$, respectively $\mathcal{T}_{h_S}$ and $\mathcal{T}_{h_V}$, are compatible in $\Gamma_{\text{coat}}$ (see the zoomed part of Figure 3). We represent by $\Delta_1$ a typical element of $\mathcal{T}_{h_S}$ and by $\Delta_2$ a typical element of $\mathcal{T}_{h_V}$.

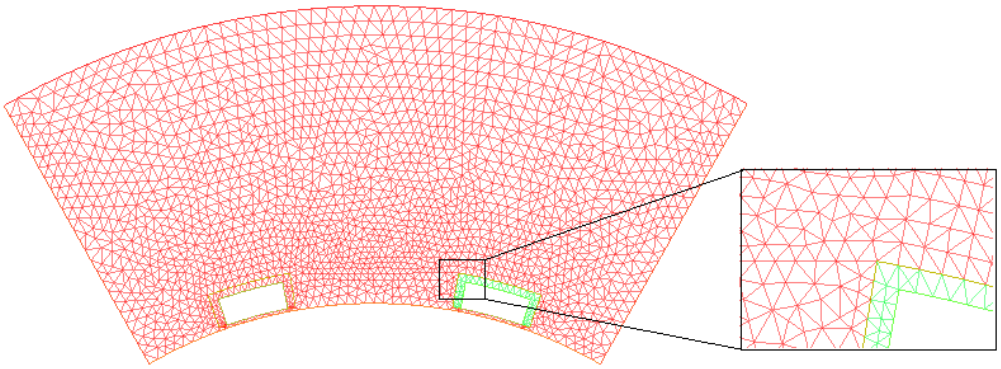

FIGURE 3. Triangulations in the stent and in the vessel wall.

Let $S_h = \bigcup_{\Delta_1 \in \mathcal{T}_{h_S}} \Delta_1$, $V_h = \bigcup_{\Delta_2 \in \mathcal{T}_{h_V}} \Delta_2$ and let $\mathcal{A}_{S,h}(.,.)$ and $\mathcal{A}_{V,h}(.,.)$ be defined as $\mathcal{A}_S(.,.)$ and $\mathcal{A}_V(.,.)$ but with the $L^2$ inner product defined on $S_h$ and $V_h$, respectively. To define the bilinear form corresponding to $a_{\text{lumen}}(.,.)$, we represent by $\Gamma_{\text{lumen},h}$ the boundary of $V_h$ that replaces $\Gamma_{\text{lumen}}$.
We assume that $p_{\text{adv}} = 0$ and $p_{\text{lumen}} = p_{0,h}$. We define in what follows the

space of globally continuous functions on $S_h$ and $V_h$ whose restrictions to each element $\Delta_1$ and $\Delta_2$ respectively, are polynomials of degree at most $n$, i.e.

$$\mathcal{V}_h = \Big\{ (p_{S,h}, p_{V,h}) \in C^0(\bar{S}_h) \times C^0(\bar{V}_h) \text{ such that } p_{S,h} = p_{V,h} \text{ on } \Gamma_{\text{coat}} \text{ and } p_{V,h} = 0 \text{ on } \Gamma_{\text{lumen}} \\ \text{and } (p_{S,h}, p_{V,h})\big|_{\Delta_1 \times \Delta_2} \in P_n \times P_n, \text{ for all } \Delta_1 \in \mathcal{T}_{h_S} \text{ and } \Delta_2 \in \mathcal{T}_{h_V} \Big\} \subset H^1(S_h) \times H^1_{\text{lumen}}(V_h). \tag{45}$$

In (45), $P_n$ denotes the space of polynomial of degree at most $n$.
The finite dimensional formulation for system (25) reads:
Find $(p_{S,h}, p^*_{V,h}) \in \mathcal{V}_h$ such that

$$\mathcal{A}_{S,h}(p_{S,h}, q_{S,h}) + \mathcal{A}_{V,h}(p^*_{V,h}, q_{V,h}) = -\mathcal{A}_{V,h}(w_h, q_{V,h}), \ \ \forall\ (q_{S,h}, q_{V,h}) \in \mathcal{V}_h. \tag{46}$$

We use in what follows the following notations

$$\big(v_{S,h}, v_{V,h}\big) = \left( \big(v_{m,S,h}\big)_{m=1,\dots,5}, \big(v_{m,V,h}\big)_{\substack{m=1,\dots,5 \\ m\neq 2}} \right). \tag{47}$$

To compute the semi-discrete Ritz-Galerkin approximation $\mathcal{C}_h = (\mathcal{C}_{S,h}, \mathcal{C}_{V,h})$ for the weak solution of $\mathcal{C} = (\mathcal{C}_S, \mathcal{C}_V)$ defined by (15) − (18) and (22), we consider the space

$$\mathcal{W}_h = \{ \Big( v_{S,h}, v_{V,h}) \in \big(C^0(\bar{S}_h)\big)^5 \times \big(C^0(\bar{V}_h)\big)^4 \text{ such that } v_{m,S,h} = v_{m,V,h} \text{ on } \Gamma_{\text{coat}},\ m = 1,3,4,5 \\ \text{and } (v_{S,h}, v_{V,h})\big|_{\Delta_1 \times \Delta_2} \in (P_q)^5 \times (P_q)^4 \text{ for all } \Delta_1 \in \mathcal{T}_{h_S} \text{ and } \Delta_2 \in \mathcal{T}_{h_V} \Big\} \subset \big(H^1(S_h)\big)^5 \times \big(H^1(V_h)\big)^4, \tag{48}$$

where $P_q$ denotes the space of polynomial of degree at most $q$ (not necessarily equal to $n$).
By $a_{j,h}(.,.)$ we represent the bilinear form defined on $a_j(.,.)$ but with the $L^2$ inner products defined on $S_h$ for $j = S$ and $V_h$ for $j = V$. By $a_{\text{lumen},h}(.,.)$ we denote the bilinear form defined as $a_{\text{lumen}}(.,.)$ but considering the boundary integrals on $\Gamma_{\text{lumen},h}$.
The weak solution of the problem (15) − (18) and (22) in the discrete case is the solution of the following finite dimensional variational formulation:
Find $\big(\mathcal{C}_{S,h}, \mathcal{C}_{V,h}\big) \in L^2(0,T,\mathcal{W}_h)$ such that $(\frac{\partial \mathcal{C}_{S,h}}{\partial t}, \frac{\partial \mathcal{C}_{V,h}}{\partial t}) \in \Big( L^2(0,T; L^2(S_h)) \Big)^5 \times \Big( L^2(0,T; L^2(V_h)) \Big)^4$ and

$$\begin{cases} \displaystyle\sum_{j=S,V} \Big( \big(\tfrac{\partial \mathcal{C}_{j,h}}{\partial t}(t), v_{j,h}\big)_{j,h} + a_{j,h}\big(\mathcal{C}_{j,h}(t), v_{j,h}\big) \Big) = \sum_{j=S,V} \big(\mathcal{F}_j(\mathcal{C}_{j,h}(t)), v_{j,h}\big)_{j,h} + a_{\text{lumen},h}(\mathcal{C}_{V,h}(t), v_{V,h}), \\ \text{a.e in } (0,T), \text{ for all } (v_{S,h}, v_{V,h}) \in \mathcal{W}_h, \\ \mathcal{C}_{S,h}(0) = (0,1,0,0,1),\ \mathcal{C}_{V,h}(0) = (1,0,0,0). \end{cases} \tag{49}$$

To conclude this section, we introduce the semi-discrete energy functional

$$\mathcal{E}_h(t) = \sum_{j=S,V} \left( \left\| \mathcal{C}_{j,h}(t) \right\|^2_{L^2(j)} + \int_0^t \left\| \nabla \mathcal{C}_{j,h}(s) \right\|^2_{L^2(j)} ds \right) + \left\| \int_0^t e^{-\frac{t-s}{\tau_1}} \nabla \mathcal{C}_{V,h}(s) ds \right\|^2_{L^2(V)}, \quad (50)$$

where $t \in [0,T]$ and $\mathcal{C}_{j,h}(t),\ j = S,V$, is the solution of (49).
This functional is the semi-discrete version of the energy functional (35). Following a procedure analogous to the one in Theorem 4.1, a discrete version of inequality (37) can be established.

## 6. *Numerical Results*

All experiments have been carried out with the open source PDE solver freeFEM++ considering the triangulation plotted in Figure 3, with 3688 elements (1968 vertices) for the vessel wall and 100 elements (83 vertices) for each stent. The time integration of (49) has been performed using an implicit-explicit backward formula in the time grid $\left\{ t_n; n = 0, 1, \ldots, N \right\}$, $t_0 = 0, t_N = T$ and with time step size $\Delta t = 10^{-3}$.
The IMEX method is defined by integrating (49) with an implicit Euler method where the diffusion and the convective terms are considered implicitly being the diffusion coefficients explicit. In the discretization of the reaction terms, we adopt an implicit-explicit approach which convert each nonlinear reaction into a linear one. To compute the finite element solutions of problem (49) we need to evaluate some convolution integrals. To avoid the use of quadrature rules we generate and implicitly solve a set of ordinary differential equations which solutions are those integrals.
Several choices of finite element spaces can be made, but we use here the piecewise linear finite element space $P_1$ for concentrations and quadratic finite element space $P_2$ for the pressure drop.
We define the mass in the coated stent and in the vessel wall by

$$\begin{aligned} \mathcal{M}_{m,S,h}(t) &= \int_{S_h} C_{m,S,h}(t) dS,\ m = 1, \ldots, 5, \\ \mathcal{M}_{m,V,h}(t) &= \int_{V_h} C_{m,V,h}(t) dV,\ m = 1, \ldots, 5,\ m \neq 2, \end{aligned} \quad (51)$$

respectively.
The following values for the parameters, extracted from [21, 22], and [31],

have been considered in the numerical experiments.

$$\kappa_{1,S} = \kappa_{2,V} = 1 \times 10^{-6}\ cm^2/g.s,\ \kappa_{2,S} = 1 \times 10^{-7}\ cm^2/g.s,\ \gamma_{m,V} = 1 \times 10^{10}\ cm/s,$$
$$D^0_{1,S} = 1 \times 10^{-8}\ cm^2/s, D^0_{2,S} = 1 \times 10^{-15}\ cm^2/s,\ D^0_{3,S} = 1 \times 10^{-10}\ cm^2/s,$$
$$D^0_{4,S} = 2 \times 10^{-10}\ cm^2/s,\ D^0_{5,S} = 1 \times 10^{-8}\ cm^2/s,\ k_S = 2 \times 10^{-14}\ cm^2,$$
$$k_V = 1 \times 10^{-15}\ cm^2,\ \mu_S = 0.72 \times 10^{-2}\ g/cm.s, \mu_V = 0.5 \times 10^{-2}\ g/cm.s,$$
$$D_{1,V} = 1 \times 10^{-8}\ cm^2/s, D^0_{3,V} = 1 \times 10^{-10}\ cm^2/s,\ D^0_{4,V} = 2 \times 10^{-10}\ cm^2/s,$$
$$D^0_{5,V} = 5 \times 10^{-9}\ cm^2/s, \alpha = 1\ s/cm^2,\ \beta = \gamma = 10\ s/cm^2.$$

We set $p_{\text{lumen}} = 100$ mmHg and $p_{\text{adv}} = 0$ mmHg, so we impose a pressure difference between the inner ($\Gamma_{\text{lumen}}$) and the outer surface ($\Gamma_{\text{adv}}$) of the arterial wall. A velocity field in the coupled stent-wall system is caused by this pressure jump.
The pressure drop obtained by system (25) is shown in Figure 4 ($b$). While pressure on $\Gamma_{\text{coat}}$ is around 76.88 mmHg, it is observed that the average pressure in the vessel wall and in the stent are 35.93 mmHg and 75.34 mmHg respectively.

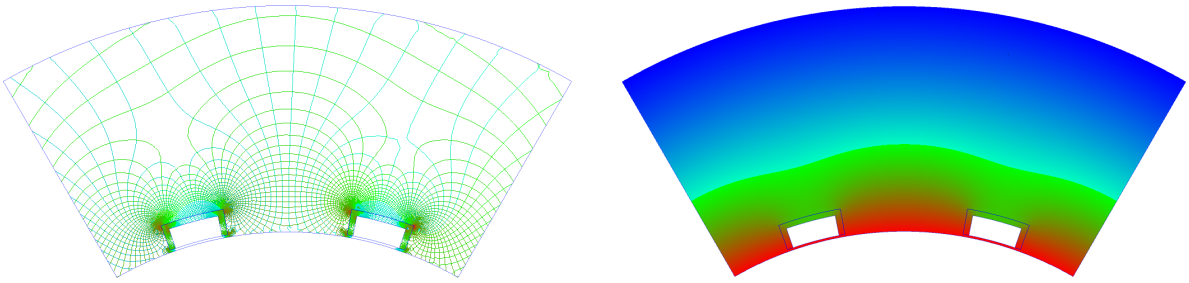

FIGURE 4. Velocity field (left) and pressure distribution (right) in the coupled system.

The release of the drug from the stent into the vessel wall is shown in Figure 5. As time evolves the mass of the drug increases in the vessel wall.

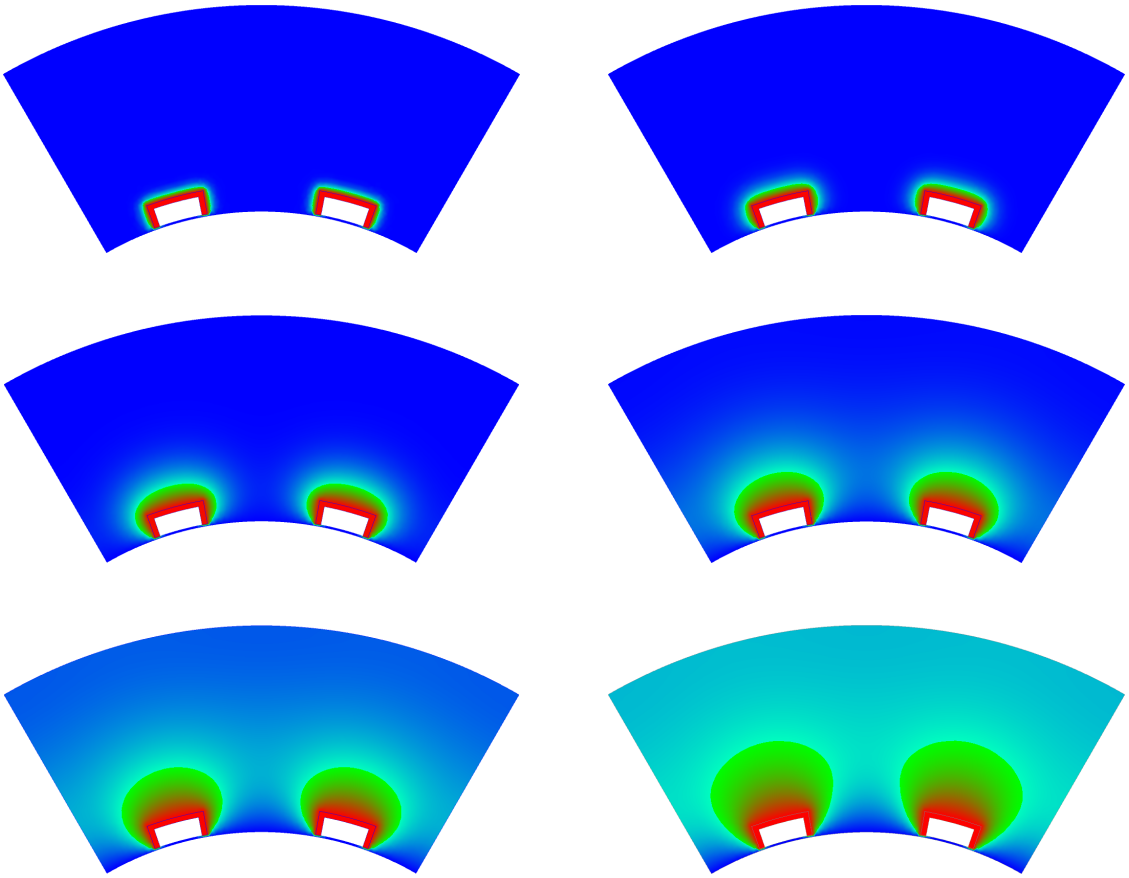

FIGURE 5. Evolution of drug distribution in the stent and the vessel wall during 6 months (left to right: 6 hours, 1 day, 1 week, 1 month, 3 and 6 months).

The behavior of the mass of drug, the mass of PLA and the amount of fluid in the biodegradable stent is shown in Figure 6. The drug presents a steep initial gradient and gradually vanishes after three months. The penetration of the fluid in the stent presents a steep initial slope and after around 20 days achieves a steady state. We can also observe in Figure 6 that as PLA degrades, the release rate of drug decreases.
The release of drug from a biodegradable stent and a non-biodegradable stent are compared in Figure 7. We observe that due to degradation of the polymer, the drug release from a biodegradable stent is faster than the drug release from a non-biodegradable stent. The drug release rate directly depends on the reaction rate $\kappa_{1,S}$.

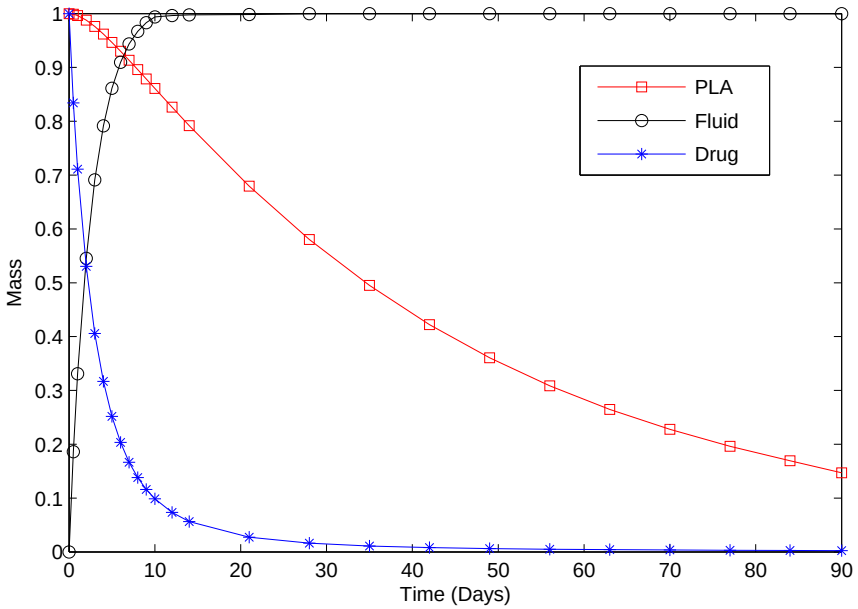


FIGURE 6. Mass behaviour of fluid, PLA and drug in the stent during 90 days.

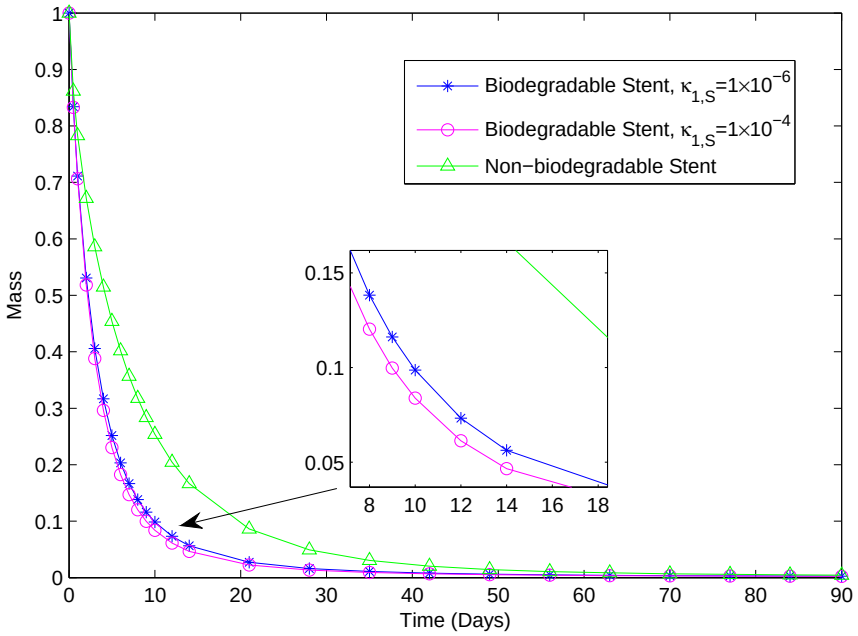


FIGURE 7. Mass of drug in biodegradable stent versus non-biodegradable stent.

The influence of the stiffness of the vessel wall in the diffusion process of the drug is shown in Figures 8 and 9. A healthy coronary artery with Young modulus $\kappa_r = 1.2$ MPa (see [11]) is compared with a highly diseased coronary artery with Young modulus $\kappa_r = 4.1$ MPa (see [18]).

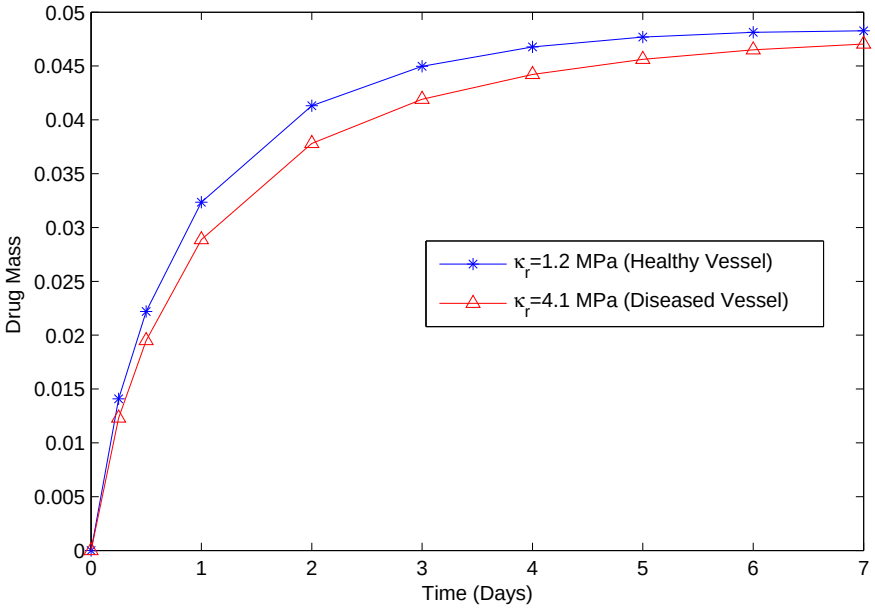


FIGURE 8. Short time effect of $\kappa_r$ on the drug mass that enters in the vessel wall, $\tau_1 = 0.5$, $\kappa_1 = 1$, 3-parameter solid model.

As $\kappa_r$ increases due to age or atherosclerosis, the vessel wall is less elastic, that is more stiff, and less drug penetrates to the coronary wall. This is an interesting finding from the medical viewpoint, because cardiovascular morbidity is related with arterial stiffness [12]. It means that the concentration of drug in the DES should be tailored to the severity of the arterial disease. In the framework of our numerical experiments the drug reduction of mass in the initial days of the process could be compensated by adding 2 percent drug to the initial concentration.

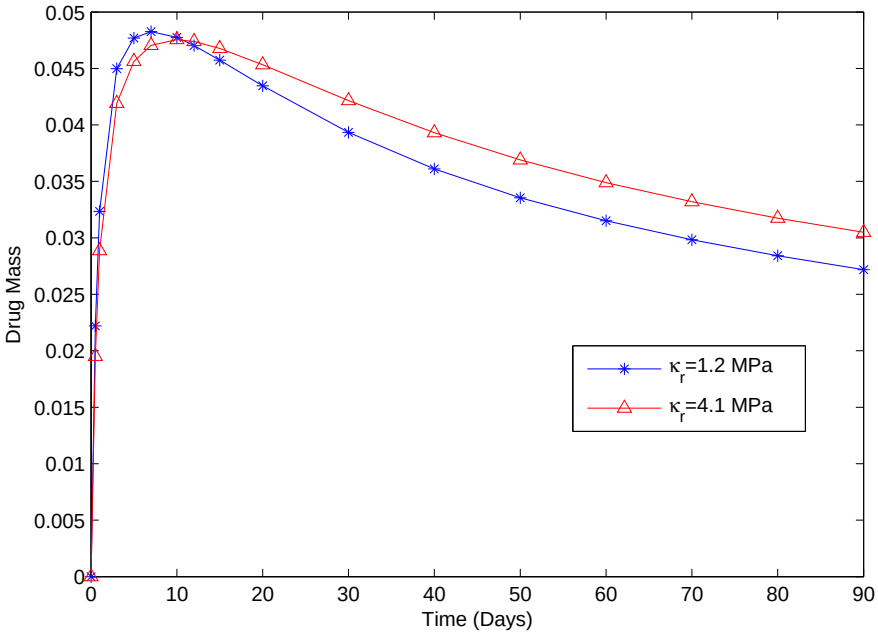


FIGURE 9. Long time effect of $\kappa_r$ on the drug mass that enters in the vessel wall,, $\tau_1 = 0.5$, $\kappa_1 = 1$, 3-parameter solid model.

The long term influence of stiffness of the coronary wall in the diffusion process of the drug is shown in Figure 9. In the beginning of the treatment, a diseased coronary wall receives less drug due to its large $\kappa_r$ when we compare with a healthy coronary wall. A crossing occurs after the initial times around day 15. This finding is justified by the fact that the stiffness of the vessel wall imposes a resistance to the penetration of the drug in the beginning of the process and leads to a drug accumulation in the long time.
When an additional thin layer named *topcoat* is applied to the PLA matrix, instead of the interface conditions (21), we consider the following interface conditions

$$\begin{cases} J_{m,S}.\eta_S = P_c(C_{m,S} - C_{m,V}), \\ J_{m,S}.\eta_S = -J_{m,V}.\eta_V, \end{cases} \tag{52}$$

for $m = 1, \ldots, 5,\ m \neq 2$, where $P_c$ is the permeability of the interface layer $\Gamma_{\text{coat}}$. The first condition in (52) is the second Kedem-Katchalsky equation (see [21] and the references therein). We remark that the topcoat is used to slow down the release rate of the drug and it gives more controllability of the drug delivery process.

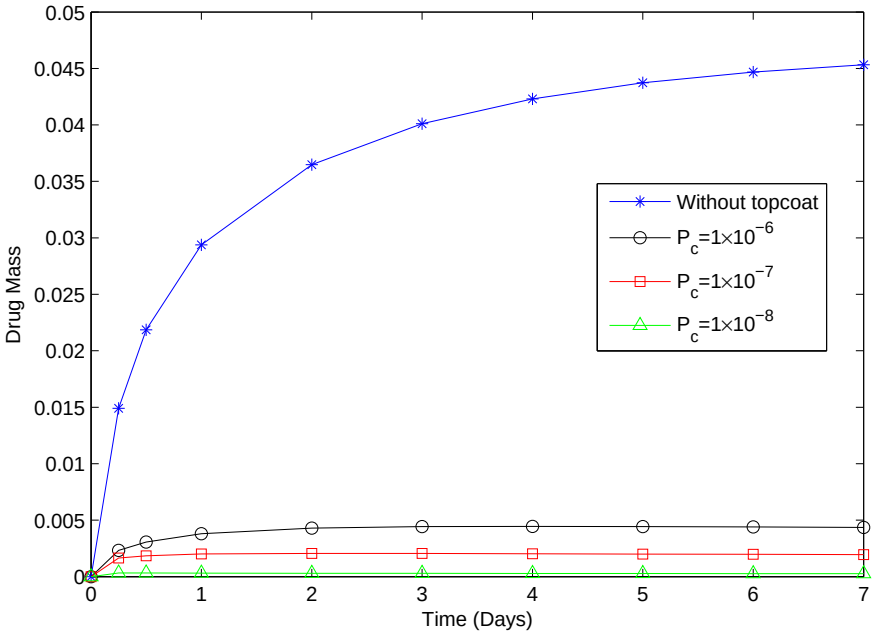


FIGURE 10. The effect of topcoat on the drug release in the vessel wall, 3-parameter solid model.

Figure 10 presents the effect of permeability of the interface layer $\Gamma_{\text{coat}}$ on the drug release when a topcoat is applied to the PLA. The accumulation of drug will decrease when a topcoat with smaller permeability is applied to the coated stent. This means that the release of drug from the stent into a vessel wall can be controlled by applying topcoats with different permeabilities.
*Fung*'s quasilinear viscoelastic model ([9]) is commonly used to describe the viscoelastic properties of the living tissues. Several authors consider that *Fung*'s quasilinear viscoleastic model is a simple method to incorporate nonlinearity and viscoelasticity and is a good model for living tissues with moderate deformation ([1, 9, 17, 29]).
The aim of this subsection is to show that the effect of the rheological properties of the vessel wall, on drug permeation, are described analogously by Maxwell-Wiechert model and Fung's model.
In the framework of Fung's model, the relation between stress and strain is given by the following convolution integral

$$\sigma_V(t) = -\int_0^t \tilde{K}(t-s)\frac{d\sigma^e(\varepsilon_V)}{ds}(s)ds, \tag{53}$$

where

$$\tilde{K}(t-s) = \frac{1 + c\int_{\tau_1}^{\tau_2} \frac{1}{\tau} e^{-\frac{t-s}{\tau}} d\tau}{1 + c\ln(\frac{\tau_2}{\tau_1})}, \tag{54}$$

and

$$\sigma^e(\varepsilon_V(t)) = \lambda_1\big(e^{\lambda_2 \varepsilon_V(t)} - 1\big) \simeq \lambda_1\lambda_2\varepsilon_V(t). \tag{55}$$

In (54), $c > 0$ represents the degree of viscous effects, $\tau_1$ and $\tau_2$ represent the short-term and long-term time constants respectively. In (55), $\sigma^e(\varepsilon_V)$ represents the instantaneous nonlinear elastic strain, $\lambda_1 > 0$ is the elastic stress constant (MPa) and $\lambda_2$ is a non-dimensional parameter representing the nonlinearity of instantaneous elastic response.
Replacing (54) and (55) into (53), we obtain

$$\sigma_V(t) = -\tilde{k}_r\bigg(\varepsilon_V(t) + c\int_0^t \int_{\tau_1}^{\tau_2} \frac{1}{\tau} e^{-\frac{t-s}{\tau}} d\tau \frac{d\varepsilon_V}{ds}(s) ds\bigg), \tag{56}$$

where $\tilde{k}_r = \frac{\lambda_1\lambda_2}{1+c\ln(\frac{\tau_2}{\tau_1})}$.
The quasilinear viscoelastic model has five material parameters (three for the reduced relaxation function ( Equation (54)) and two for the elastic response ( Equation (55)) which must be determined experimentally. Although some estimations are available in the literature for ligaments ([13]), femur-MCL-tibia complexes ([1]) and spinal tissue ([29]), to the best knowledge of the authors, physiological values of these five parameters are not available in the case of coronary walls.
Due to the lack of appropriate information, we fix four parameters $\lambda_1 = 0.2$ Mpa, $\lambda_2 = 25$, $\tau_1 = 0.5$s and $\tau_2 = 1800$s and choose $c = 0.37$ to have $\tilde{\kappa}_r = 1.2$ Mpa for healthy arterial wall ([11]) and $c = 0.02$ to have $\tilde{\kappa}_r = 4.1$ Mpa for highly diseased arterial wall ([18]).
The plots in Figures 11 and 12 show that the profile of drug release exhibits the same qualitative behavior as before. The barrier to drug permeation of stiff vessel walls, in the first period of drug delivery, is a clinical finding suggested by Fung's and Maxwell-Wiechert mechanistic models.

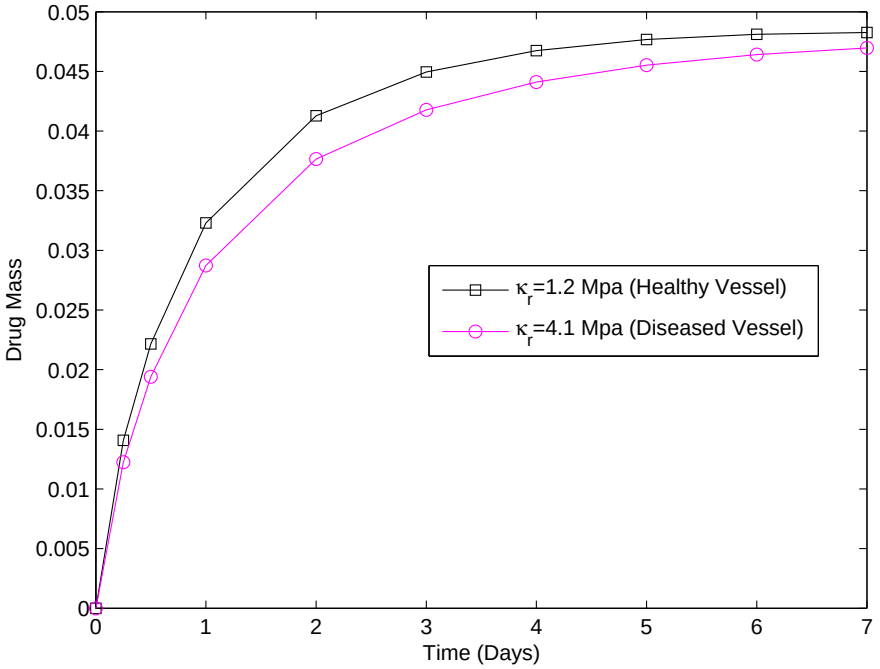


FIGURE 11. Short time effect of parameter $\tilde{\kappa}_r$ on the drug release in the vessel wall (*Fung*'s model).

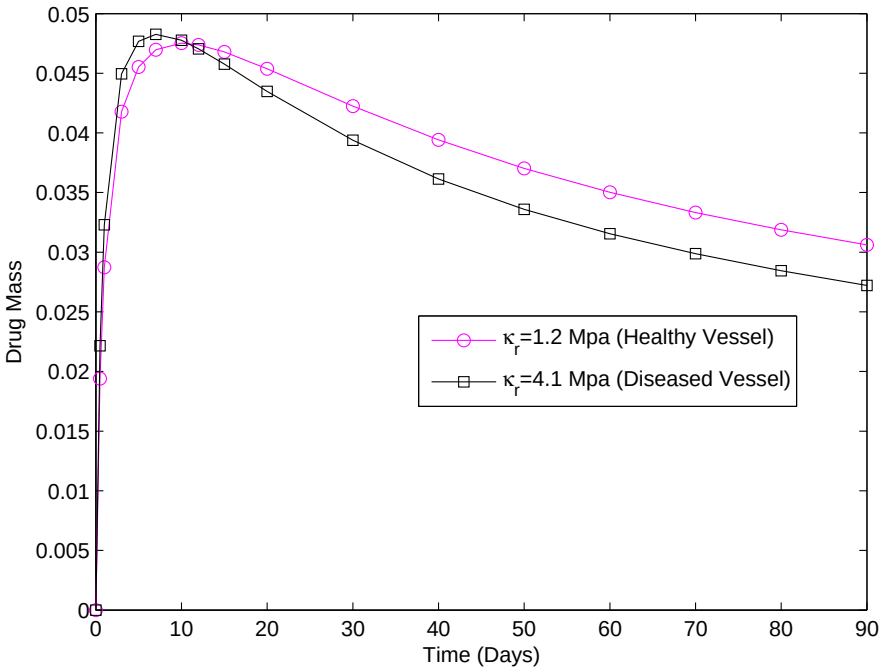


FIGURE 12. Long time effect of parameter $\tilde{\kappa}_r$ on the drug release in the vessel wall (*Fung*'s model).

## 7. *Conclusions*

In recent years mathematical modeling has become an effective tool in simulating drug delivery processes. In the case of drug eluting stents it leads to a deeper understanding of the drug release mechanisms in the biodegradable coating and in the vessel wall. Although the cardiovascular drug delivery depends on very complex biochemical and physiological phenomena, a simplified release model can help to adapt the delivery profile to patient needs. In this paper we present a coupled model to simulate drug delivery from a stent to a vessel wall. The coating of the stent is biodegradable and viscoelastic properties of the vessel wall are included in the model. From a theoretical viewpoint we prove the stability of the continuous model and the stability of a fully discrete model.

From the numerical viewpoint two particular aspects of clinical importance are addressed in the paper: the influence of the viscoelasticity of the vessel wall and the effect of permeability of the stent coating.

Concerning the first aspect we show that during an initial period of time the permeation of drug in the vessel is affected by its stiffness: the total mass of drug that enters the vessel is a decreasing function of the Young modulus. Patients who need a cardiovascular stent generally have atherosclerosis and consequently stiff vessels that have high Young modulus. To prevent an inflammatory response and the smooth muscle cell growth a correct concentration of drug must penetrate the vessel from the moment when the stent is implanted. Our findings suggest that the initial concentration of drug in the stent should be tailored to the rheological properties of the vessel walls.

The second aspect we want to stress is the control of the release profile according to the permeability of the coating: release can be speed up or delayed as different polymers are used.

# Annex

| Parameter/Variable | Unit | Equation |
|---|---|---|
| $\kappa_{1,S}, \kappa_{2,S}, \kappa_{1,V}$ | $cm^2/g.s$ | (5) |
| $\alpha, \beta, \gamma$ | $s/cm^2$ | (5) |
| $u_S, u_V$ | $cm/s$ | (6),(7) |
| $k_S, k_V$ | $cm^2$ | (6),(7) |
| $\mu_S, \mu_V$ | $g/cm.s$ | (6),(7) |
| $C_{m,S}, C_{m,V}$ | $g/cm^2$ | (13),(14) |
| $D_{m,S}, \bar{D}_{m,V}$ | $cm^2/s$ | (13),(14) |
| $\gamma_{m,V}$ | $cm/s$ | (22) |
| $P_c$ | $cm/s$ | (52) |

TABLE 2. Parameters of the model in the drug eluting stent and vessel wall.

In the column Equation, we indicate the first equation in the paper where the parameter or variable appear.

## Acknowledgements

This work was partially supported by the Centro de Matematica da Universidade de Coimbra (CMUC), funded by the European Regional Development Fund through the program COMPETE and by the Portuguese Government through the FCT under the project, PEst-C/MAT/UI0324/2013, by the project UTAustin/MAT/0066/2008 and also FCT-Grant SFRH / BD / 51167 / 2010.

## References

[1] S.D. Abramowitch, S.D., S.L. Woo, *A new analytical approach to evaluate the viscoelastic properties of the goat medial colateral ligament using the quasi-linear viscoelastic theory*, Ann. Biomed. Eng. **32(3)** (2004) 329–335.

[2] R. Adams, J. Fournier, *Sobolev spaces*, Elsevier 2nd edition, 2003.

[3] G. Acharya and K. Park, *Mechanisms of controlled drug release from drug-eluting stents*, Adv. Drug Deliver. Rev. **58(3)** (2006) 387–401.

[4] H.F. Brinson and L.C. Brinson, *Polymer Engineering Science and Viscoelasticity An Introduction*, Springer, 2008.

[5] A. Borghi, E. Foa, R. Balossino, F. Migliavacca and G. Dobini, *Modeling drug elution from stents: effect of reversible binding in the vascular wall and degradable polymeric matrix*, Comput. Meth. Biomech. Biomed. Eng. **11 (4)** (2008) 367–377.

[6] L.C. Evans, *Partial Differential Equations*, Graduate Studies in Mathematics Volume 19, American Mathematical Society, 1998.

[7] J.A. Ferreira, M. Grassi, E. Gudino, P. de Oliveira, *A 3D model for mechanistic control of drug release*, Preprint of the Department of Mathematics, Universidade de Coimbra, No. 13-42, September 25, 2013, To appear in SIAM Journal on Applied Mathematics.

[8] J.A. Ferreira, J. Naghipoor, P. de Oliveira, *Numerical simulation of a coupled cardiovascular drug delivery model*, Proceedings of the 13th International Conference on Computational and Mathematical Methods in Science and Engineering, CMMSE 2013 **(II)** (2013) 642–653.

[9] Y.C. Fung, *Biomechanics: Mechanical Properties of Living Tissues*, Springer, New York, 1993.

[10] M. Grassi, L. Teresi, G. Grassi, L.Comel, *Novel design of drug delivery in stented arteries: a numerical comparative study*, Math. Bios. Eng. **6 (3)** (2009) 493–508.

[11] BS. Gow, CD. Hadfield, *The elasticity of canine and human coronary arteries with reference to postmortem changes*, Circ. Res. **45 (5)** (1979) 588-594.

[12] T. Khamdaenga, J. Luo, J. Vappou, P. Terdtoon, E.E. Konofagou, *Arterial stiffness identification of the human carotid artery using the stress-strain relationship in vivo*, Ultrasonic **52 (3)** (2012) 402–411.

[13] M. Kohandel, S. Sivaloganathan, G. Tenti, *Estimation of the quasi-linear viscoelastic parameters using a genetic algorithm*, Ultrasonic **47 (3-4)** (2008) 266–270.

[14] F. Migliavacca, F. Gervaso, M. Prosi, P. Zunino, S. Minisini, L. Formaggia and G. Dubini, *Expansion and drug elution model of a coronary stent*, Comp. Meth. Biomech. Biom. Eng. **10 (1)** (2007) 63–73.

[15] A. Muliana, K.R. Rajagopal, *Modeling the response of nonlinear viscoelastic biodegradable polymeric stents*, Int. J. Solids and Structures **49 (7-8)** (2012) 989–1000.

[16] A. Muliana, K.R. Rajagopal, *Changes in the response of viscoelastic solids due to changes in their internal structures*, Acta Mech. **207(3-4)** (2011) 297–316.

[17] A. Nekouzadeh, K.M. Pryse, E.L. Elson, G.M. Genin, *A simplified approach to quasi-linear viscoelastic modeling*, J. Biomech. **40 (14)** (2007) 3070-3078.

[18] I. Ozolanta, G. Tetere, B. Purinya, V. Kasyanov, *Changes in the mechanical properties, biochemical contents and wall structure of the human coronary arteries with age and sex*, Med. Eng. Phys. **20 (7)** (1998) 523–533.

[19] G. Pontrelli, F. de Monte, *Mass diffusion through two-layer porous media: an application to the drug-eluting stent*, Int. J. Heat Mass Tran. **50 (17-18)** (2007) 3658–3669.

[20] G. Pontrelli, F. de Monte, *Modelling of mass dynamics in arterial drug-eluting stents*, J. Porous Media **12 (1)** (2009) 19–28.

[21] G. Pontrelli, F. de Monte, *A multi-layer porous wall model for coronary drug-eluting stents*, J. Porous Media **53 (19-20)** (2010) 3629-3637.

[22] S. Prabhu, S. Hossainy, *Modeling of degradation and drug release from a biodegradable stent coating*, J. Biomed. Mater. Res. **80(3)** (2007) 732–741.

[23] A. Raval, J. Parikh, C. Engineer, *Mechanism of controlled release kinetics from medical devices*, Braz. J. Chem. Eng. **27 (19-20)** (2010) 211–225.

[24] P.W. Serruys, A.H. Gershlick, *Handbook of Drug eluting stent*, CRC Press; 1st edition, 2005.

[25] J. Siepmann, A. Gopferich, *Mathematical modeling of bioerodible polymeric drug delivery systems*,Adv. Drug Delivery Rev. **48 (2-3)** (2001) 229–248.

[26] J.S. Soares, *Constitutive Modeling for Biodegradable Polymers for Applications in Endovascular Stents, PhD Dissertation*, Mechanical Engineering Texas A&M University, 2008

[27] J.S. Soares, J.E. Moore,, K.R. Rajagopal,*Modeling of deformation accelerated breakdown of polylactic acid biodegradable stents.* ASME J. Med. Sci. **4(4)**(2010) 041007

[28] Y. Tao, *Nonlinear Viscoelastic Properties and Constitutive Modeling of Blood Vessel, Master Dissertation*, Mechanical Engineering National University of Singapore, 2009.
[29] K.L. Troyer, D.J. Estep, C.M. Puttlitz, *Viscoelastic effects during loading play an integral role in soft tissue mechanics*, Acta Biomat. **8 (1)** (2012) 234–243.
[30] C. Vergara, P. Zunino, *Multiscale boundary conditions for drug release from cardiovascular stents*, Mult. Model Sim. **7 (2)** (2008) 565–588.
[31] P. Zunino, *Multidimensional pharmacokinetic models applied to the design of drug-eluting stents*, Cardiov. Eng. Int. J. **4 (2)** (2004) 181–191.

J.A. Ferreira
CMUC-Department of Mathematics, University of Coimbra, Apartado 3008, 3001-454 Coimbra, Portugal
*E-mail address*: ferreira@mat.uc.pt
*URL*: http://www.mat.uc.pt/~ferreira

J. Naghipoor
CMUC-Department of Mathematics, University of Coimbra, Apartado 3008, 3001-454 Coimbra, Portugal
*E-mail address*: jahed@mat.uc.pt

Paula de Oliveira
CMUC-Department of Mathematics, University of Coimbra, Apartado 3008, 3001-454 Coimbra, Portugal
*E-mail address*: poliveir@mat.uc.pt
*URL*: http://www.mat.uc.pt/~poliveir